2355

Ancient Monuments Laboratory
Report 63/93

ARCHAEOMAGNETIC DATING:
LITTLE BIRCHES, WOLSELEY
STAFFORDSHIRE

P Linford

Ancient Monuments Laboratory Report 63/93

ARCHAEOMAGNETIC DATING: LITTLE BIRCHES, WOLSELEY STAFFORDSHIRE

P Linford

Summary

The remains of two furnaces, associated with a glassmaking process, at Little Birches near Wolseley in Staffordshire were sampled for archaeomagnetic dating. Whilst disturbance to one of the features since its last firing made archaeomagnetic dating impossible, the other produced a late medieval date of good precision despite reaching only low temperatures during its operation.

Author's address :-

P Linford

Ancient Monuments Laboratory
English Heritage
23 Savile Row
London
W1X 2HE

Archaeomagnetic Dating: Little Birches, Wolseley, Staffordshire.

Introduction

Excavations of a medieval glassmaking site on the northern edge of Rugeley Quarry uncovered the remains of several furnaces associated with the process. Samples were collected for archaeomagnetic dating from context 32 of furnace LBW9 by Neil Linford of the Ancient Monuments Laboratory on the 12th of November 1991; the dating project was given AML code 1LBW. A second visit was made by Neil and Paul Linford on the 27th July 1992 to collect samples from annealing furnace F7, also for archaeomagnetic dating; this project was give AML code 2LBW. Laboratory measurement and evaluation for both projects was conducted by the author.

Method

Samples were collected using the disc method (see appendix, section 1a) and orientated to True North with a gyro-theodolite. Twenty samples were recovered from feature 1LBW, all were of sandy, orange-red clay that had been baked hard by the firing of the furnace. Evidence of cracking and slumping of the structure was apparent and it was not possible to distinguish which areas had been least affected, so samples were taken from all parts that appeared well fired.

Feature 2LBW was constructed from tiles held together with a clay lining. Twenty four samples were collected from this lining, all plastic in consistency and of orange-red colouration. No evidence of damage to the feature since it was last fired was obvious.

Results

All the measurements discussed below were made using the equipment described in section 2 of the appendix.

Feature 1LBW

On inspection samples 1LBW02, 1LBW11 and 1LBW12 were considered too small to produce reliable measurements and were excluded from further analysis. Measurements of the directions of Natural Remanent Magnetisation (NRM) of the remaining samples are tabulated in table 1; the corrections discussed in sections 3b and 3c of the appendix have been applied. A graphical representation of the distribution of these directions is shown in figure 1.

From this figure it can be seen that the NRM directions of the individual samples form a broad scatter with little indication of any clustering. Two of the samples, 1LBW01 and 1LBW06 have NRM directions that do not fall within the graph area. Although the intensity of magnetisation in most of the samples is consistent with firing to above the blocking temperature, the observed scattering of NRM directions is clearly anomalous. Viscous remanence may be to blame but disturbance of the feature since its last firing must also be considered.

The scattering of the NRM directions is too great to allow a valid mean thermoremanent direction to be determined. So, to establish whether viscous remanence was the cause, two samples, 1LBW10 and 1LBW15, were partially demagnetised in 2mT increments, to a value of 30mT (see appendix, section 2b). They were then further demagnetised in 4mT increments to 50mT; sample 1LBW10 still had significant magnetisation remaining so its demagnetisation was continued to 100mT.

Measurements of the remaining thermoremanent magnetisation at each stage are tabulated in tables 2 and 3 respectively. The decline in intensity of magnetisation with increasing AF demagnetisation for each is plotted in figures 3 and 5; the variation in the remanent direction is shown in figures 4 and 6.

Neither figure 2 nor figure 4 exhibits the smooth reverse "S" shape characteristic of magnetisation normally distributed across the coercivity spectrum; indeed magnetisation appears to be more linearly distributed with increasing coercivity of remanence. Thus, the magnetisation is likely to be unstable, possibly because the samples were not heated to their blocking temperature. Such samples are likely to be affected by viscous remanence and inspection of figures 3 and 5 does show that both samples converged on a more stable thermoremanent direction after partial demagnetisation beyond 6mT.

On the strength of the above, it was decided to remeasure the thermoremanent directions of all samples after partial demagnetisation to 10mT. Measurements of these directions are tabulated in table 4; the corrections discussed in sections 3b and 3c of the appendix have been applied. A graphical representation of the distribution of these directions is shown in figure 6.

Directions of samples 1LBW01, 1LBW05, 1LBW06, 1LBW07 and 1LBW11 could not be plotted as they lie beyond the graph area; more samples are affected by this problem than for the NRM measurements, lending further weight to the assertion that the magnetisation is unstable. Most of the remaining samples still have widely scattered directions and it is likely they were not heated to a temperature high enough to acquire stable magnetisation. Five of the samples, 1LBW13, 1LBW15, 1LBW16, 1LBW17 and 1LBW18 do form a tight cluster and notably they were all taken from the same part of the furnace. Whilst these samples were well fired their directions unfortunately lie well away from any possible area on the calibration curve; demonstrating that the furnace has been subject to disturbance since its last firing. Hence, it was concluded that the feature could not be dated using archaeomagnetism.

Feature 2LBW

Measurements of the directions of Natural Remanent Magnetisation (NRM) of the samples are tabulated in table 4; the corrections discussed in sections 3b and 3c of the appendix have been applied. A graphical representation of the distribution of these directions is shown in figure 7. The NRM directions of samples 2LBW01, 2LBW03, 2LBW05, 2LBW19 and 2LBW23 are not represented in figure 7 as they lie beyond the graph area.

From this figure it can be seen that the NRM directions of the individual samples are scattered but do form a loose cluster centred around a point with dec = 10 and inc = 65. The intensity of magnetisation in most of the samples was low suggesting that they may not have experienced temperatures high enough to cause total realignment of their magnetic domains.

The scattering of the NRM directions is too great to allow a valid mean thermoremanent direction to be determined. However, it was considered likely that viscous remanence was corrupting the thermoremanent measurements and that removal of this component would improve the distribution of directions. To this end, pilot demagnetisation was carried out on sample 2LBW07; the sample being partially demagnetised in 2mT increments, to a value of 30mT (see appendix, section 2b).

Measurements of the remaining thermoremanent magnetisation at each stage is tabulated in table 5. The decline in intensity of magnetisation with increasing AF demagnetisation is plotted in figure 7; the variation in the remanent direction is shown in figure 8.

Figure 7 reveals that the magnetisation is concentrated in low coercivity domains, supporting the assertion that the samples were not heated above their blocking temperature in the operation of the furnace. Inspection of figure 8 reinforces this conclusion, showing that the direction of remanence becomes more erratic with increasing demagnetisation. In such cases the viscous component of the remanence often has a significant effect on the measured thermoremanent direction. Hence, it was decided to remeasure all samples after they had been partially demagnetised in a 4mT field, in the hope of removing this component. Measurements of these directions are tabulated in table 6; the corrections discussed in sections 3b and 3c of the appendix have been applied.

A graphical representation of the distribution of these directions is shown in figure 9. The thermoremanent directions of 2LBW01, 2LBW03, 2LBW05, 2LBW17, 2LBW20 and 2LBW23 are not represented as they lay beyond the graph area. The remaining samples form an acceptable cluster and a mean thermoremanent direction was calculated from them. Samples 2LBW10, 2LBW14 and 2LBW19 appeared to be statistical outliers and on inspection were found to have partially disintegrated during the consolidation process; they were thus excluded from this calculation. Samples lying beyond the graph area were also excluded, it being considered that no true thermoremanent signal remained in them owing to the low firing temperature that they experienced. The resulting mean was:

Dec = 11.390 +/- 2.366°; Inc = 66.609 +/- 0.939°
Alpha-95 = 1.720°

This mean was calibrated (see appendix, note 4) to produce a date range of:

1533 - 1557 cal AD at the 68% confidence level.
1521 - 1565 cal AD at the 95% confidence level.

Conclusions

The magnetic measurements made on feature 1LBW show that whilst the structure was adequately heated during operation to obtain a thermoremanent magnetisation, disturbance since its last firing made archaeomagnetic dating impossible. Measurements made on feature 2LBW show that the temperatures reached by the annealing process were not high enough to cause total realignment of the magnetic domains in the clay lining sampled. The magnetisation induced was thus unstable but, after partial demagnetisation, it was possible to obtain a satisfactory archaeomagnetic date and this is quoted above.

Paul Linford
Archaeometry Branch
Science and Conservation Services, RPS

24th June 1993

Table 1; Corrected NRM measurements for feature 1LBW.

Sample	Declination (deg)	Inclination (deg)	Intensity (Am^2x10^{-8})
1LBW01	-57.798	66.318	632.210
1LBW03	25.023	64.212	496.660
1LBW04	4.096	60.819	230.236
1LBW05	11.472	58.154	29.498
1LBW06	-67.477	62.584	45.516
1LBW07	39.452	77.388	19.263
1LBW08	38.049	59.673	65.192
1LBW09	13.063	57.327	59.231
1LBW10	10.054	66.079	126.269
1LBW13	-17.688	62.370	938.412
1LBW14	-9.921	72.037	453.177
1LBW15	-8.664	60.401	52.378
1LBW16	-11.380	63.435	132.533
1LBW17	-8.485	64.662	749.004
1LBW18	-11.486	68.281	277.696
1LBW19	-14.377	58.884	169.856
1LBW20	-27.001	63.019	545.411

Table 2; Variation of remanent field with increasing partial demagnetisation for sample 1LBW10.

Demagnetisation (mT)	Declination (deg)	Inclination (deg)	Intensity (M/M_O)
0	15.103	66.228	1.000
2	12.518	65.866	0.976
4	12.156	65.821	0.969
6	11.828	65.644	0.942
8	11.794	65.431	0.932
10	10.992	65.522	0.910
12	10.913	65.292	0.894
14	10.978	65.154	0.875
16	11.139	65.702	0.858
18	11.039	65.583	0.844
20	10.322	65.419	0.818
24	9.401	65.648	0.785
28	12.421	65.242	0.747
32	11.828	65.532	0.706
36	12.444	65.392	0.665
40	12.847	65.164	0.625
44	11.210	65.611	0.577
48	13.053	65.616	0.538
52	13.365	65.118	0.501
56	12.049	65.197	0.468
60	11.120	65.067	0.424
64	10.241	65.026	0.391
68	14.574	65.771	0.353
76	13.559	64.279	0.301
84	9.104	63.488	0.251
92	10.014	64.410	0.197
100	13.808	66.564	0.156

Table 3; Variation of remanent field with increasing partial demagnetisation for sample 1LBW15.

Demagnetisation (mT)	Declination (deg)	Inclination (deg)	Intensity (M/M_O)
0	-23.415	60.753	1.000
2	-19.553	60.534	0.956
4	-14.546	61.926	0.908
6	-12.128	61.186	0.872
8	-12.496	61.829	0.818
10	-11.990	61.668	0.781
12	-10.887	62.230	0.747
14	-11.050	62.857	0.708
16	-11.226	61.968	0.693
18	-11.450	60.894	0.655
20	-10.354	62.975	0.652
22	-8.961	63.226	0.634
24	-11.931	62.037	0.620
26	-10.852	62.853	0.594
28	-14.313	60.543	0.596
30	-11.994	61.572	0.580
34	-10.637	60.121	0.573
38	-15.139	61.491	0.550
42	-13.398	59.251	0.511
46	-12.072	58.542	0.495
50	-15.237	58.542	0.482

Table 4; Corrected measurements for feature 1LBW after 10mT AF partial demagnetisation.

Sample	Declination (deg)	Inclination (deg)	Intensity (Am^2x10^{-8})
1LBW01	-55.742	67.331	577.822
1LBW03	14.984	62.067	485.650
1LBW04	-1.536	59.240	134.378
1LBW05	16.952	47.043	19.482
1LBW06	-72.624	59.033	34.217
1LBW07	45.836	14.697	8.525
1LBW08	42.455	58.024	59.314
1LBW09	17.733	56.565	55.656
1LBW10	10.992	65.522	114.839
1LBW13	-13.741	62.801	761.243
1LBW14	-9.806	71.277	438.358
1LBW15	-11.990	61.668	42.505
1LBW16	-10.003	64.704	117.969
1LBW17	-11.166	63.864	465.241
1LBW18	-10.186	65.031	156.941
1LBW19	-16.078	52.470	62.162
1LBW20	-26.480	62.232	493.028

Table 5; Corrected NRM measurements for feature 2LBW.

Sample	Declination (deg)	Inclination (deg)	Intensity (Am^2x10^{-8})
2LBW01	66.224	82.048	11.875
2LBW02	4.460	65.905	45.861
2LBW03	-9.897	48.949	11.808
2LBW04	-0.701	71.458	14.647
2LBW05	31.436	35.243	113.939
2LBW06	20.347	61.866	29.732
2LBW07	13.119	63.636	102.971
2LBW08	11.597	74.080	46.989
2LBW09	14.152	69.632	17.783
2LBW10	-12.694	77.193	29.162
2LBW11	8.661	63.262	46.695
2LBW12	-0.350	64.808	53.354
2LBW13	13.653	66.688	142.873
2LBW14	24.258	78.404	14.970
2LBW15	4.752	69.180	24.297
2LBW16	15.942	71.487	22.616
2LBW17	1.840	52.924	12.805
2LBW18	17.170	69.498	26.230
2LBW19	23.090	43.732	23.311
2LBW20	44.961	76.462	26.845
2LBW21	11.409	73.038	28.170
2LBW22	-6.986	72.923	21.839
2LBW23	1.179	85.237	17.697
2LBW24	13.437	63.214	739.659

Table 6; Variation of remanent field with increasing partial demagnetisation for sample 2LBW07.

Demagnetisation (mT)	Declination (deg)	Inclination (deg)	Intensity (M/M_O)
0	14.282	64.276	1.000
2	13.801	60.994	0.876
4	13.405	63.013	0.714
6	11.208	62.156	0.569
8	12.986	62.347	0.478
10	10.762	66.552	0.333
12	13.910	62.059	0.292
14	18.503	64.741	0.188
16	13.865	68.898	0.170
18	7.846	66.660	0.072
20	5.933	68.983	0.076
22	26.855	59.930	0.098
24	12.241	67.705	0.162
26	12.755	64.350	0.151
28	20.465	71.284	0.135
30	3.683	68.785	0.134

Table 7; Corrected measurements for feature 2LBW after 4mT AF partial demagnetisation.

Sample	Declination (deg)	Inclination (deg)	Intensity ($Am^2 x10^{-8}$)
2LBW01	82.241	75.568	8.425
2LBW02	9.540	67.000	28.503
2LBW03	-3.170	47.328	10.659
2LBW04	3.879	69.615	10.721
2LBW05	35.664	28.491	101.579
2LBW06	15.374	62.958	22.652
2LBW07	13.405	63.013	83.359
2LBW08	13.431	72.972	36.234
2LBW09	13.522	66.495	14.801
2LBW10	-8.032	74.948	22.183
2LBW11	12.160	60.700	36.481
2LBW12	5.047	65.057	41.926
2LBW13	13.638	67.915	138.944
2LBW14	4.736	75.501	11.138
2LBW15	4.984	68.179	18.162
2LBW16	19.612	67.084	16.718
2LBW17	-0.422	49.728	11.374
2LBW18	13.111	66.203	20.326
2LBW19	6.604	53.905	34.498
2LBW20	72.397	66.689	18.723
2LBW21	12.750	68.020	21.075
2LBW22	5.328	69.861	17.503
2LBW23	19.291	82.331	13.051
2LBW24	12.888	63.186	687.103

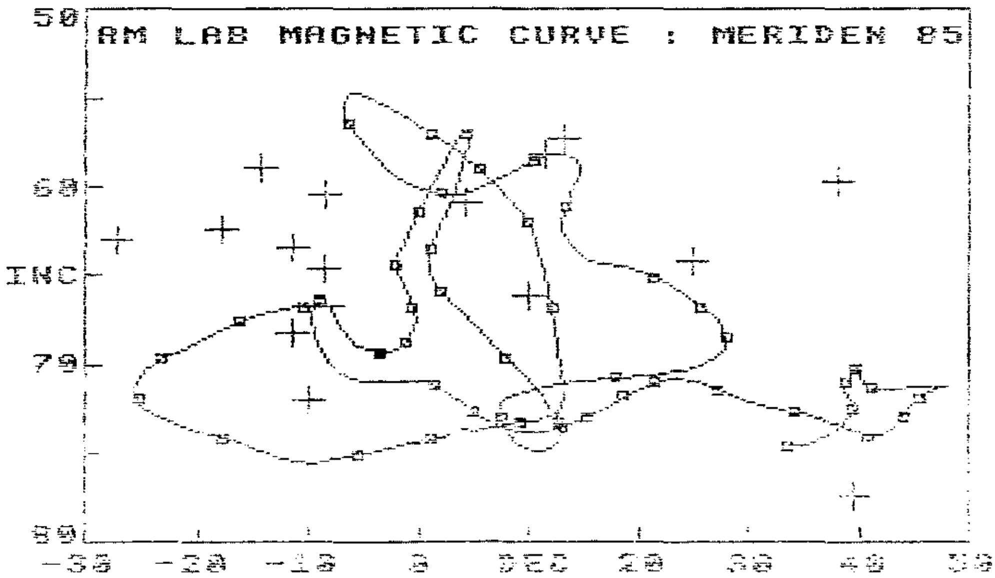

Figure 1; Distribution of NRM results from feature 1LBW.

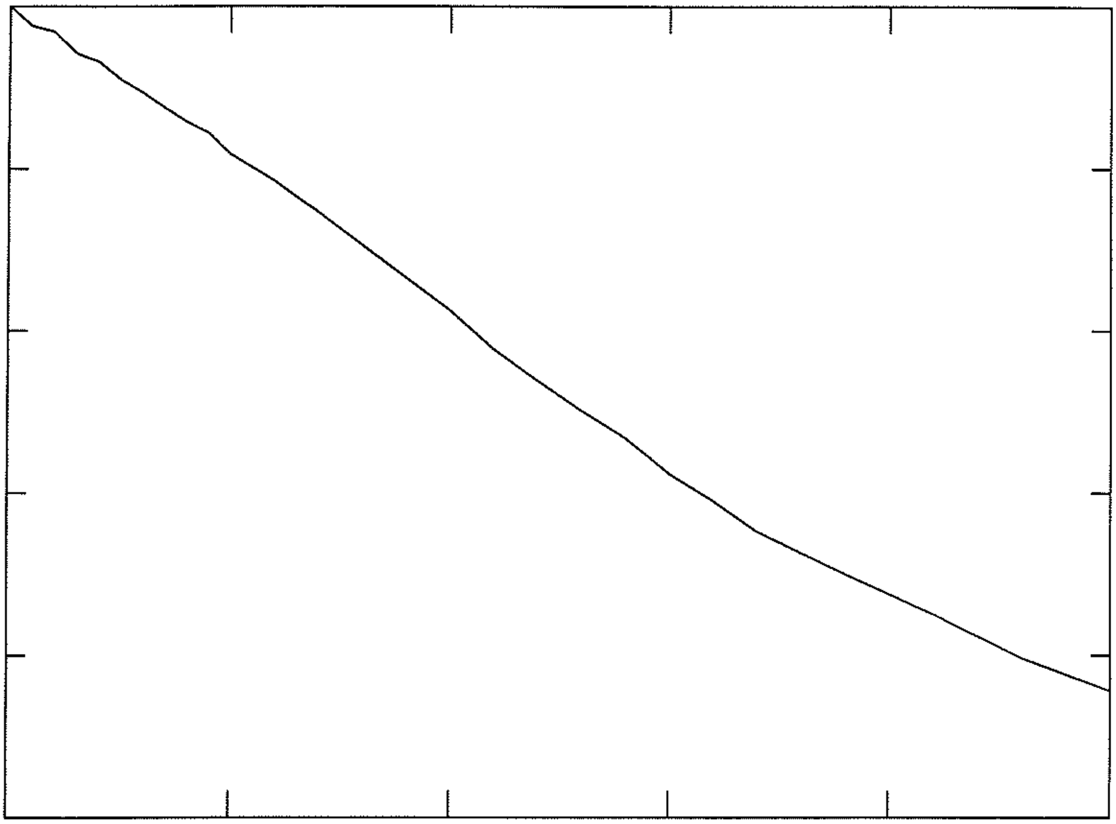

0 -x- 100 0 -y- 1

Figure 2; Variation of remanence intensity (y axis), M/Mo, with increasing partial demagnetisation in mT (x axis) for sample 1LBW10.

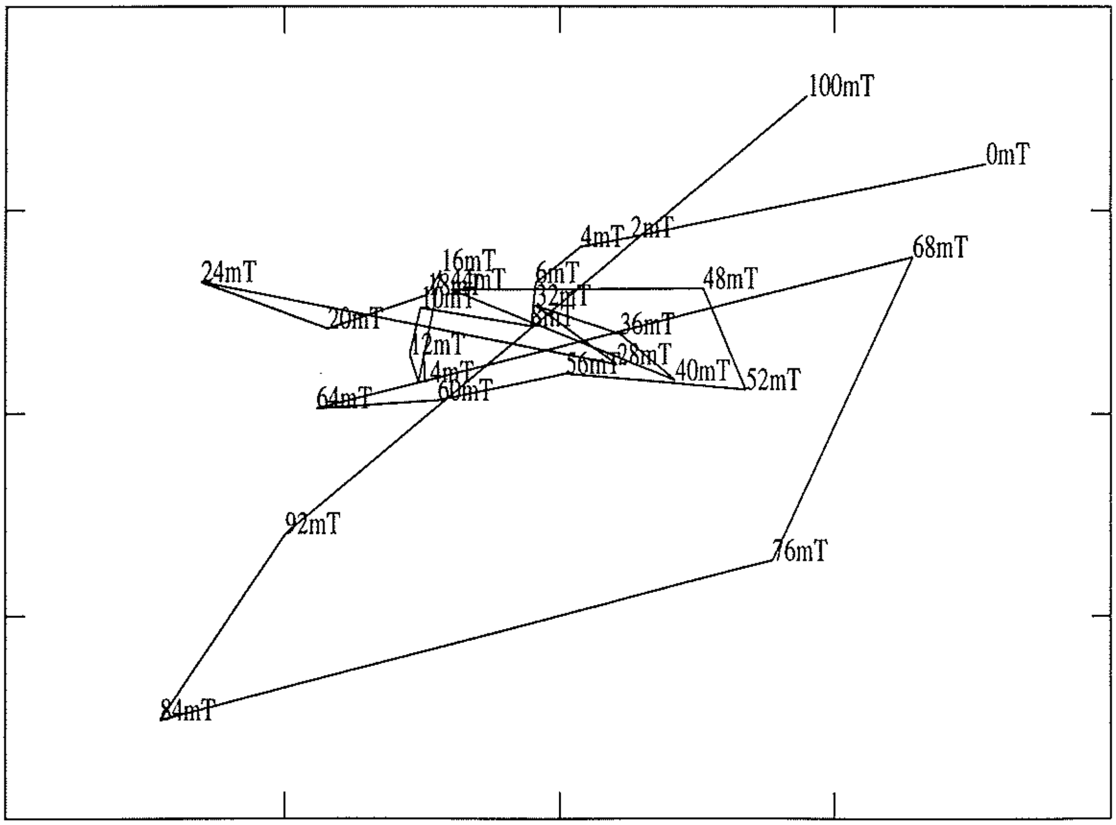

8 -x- 16 63 -y- 67

Figure 3; Variation of Dec (x axis) and Inc (y axis) with increasing partial demagnetisation for sample 1LBW10.

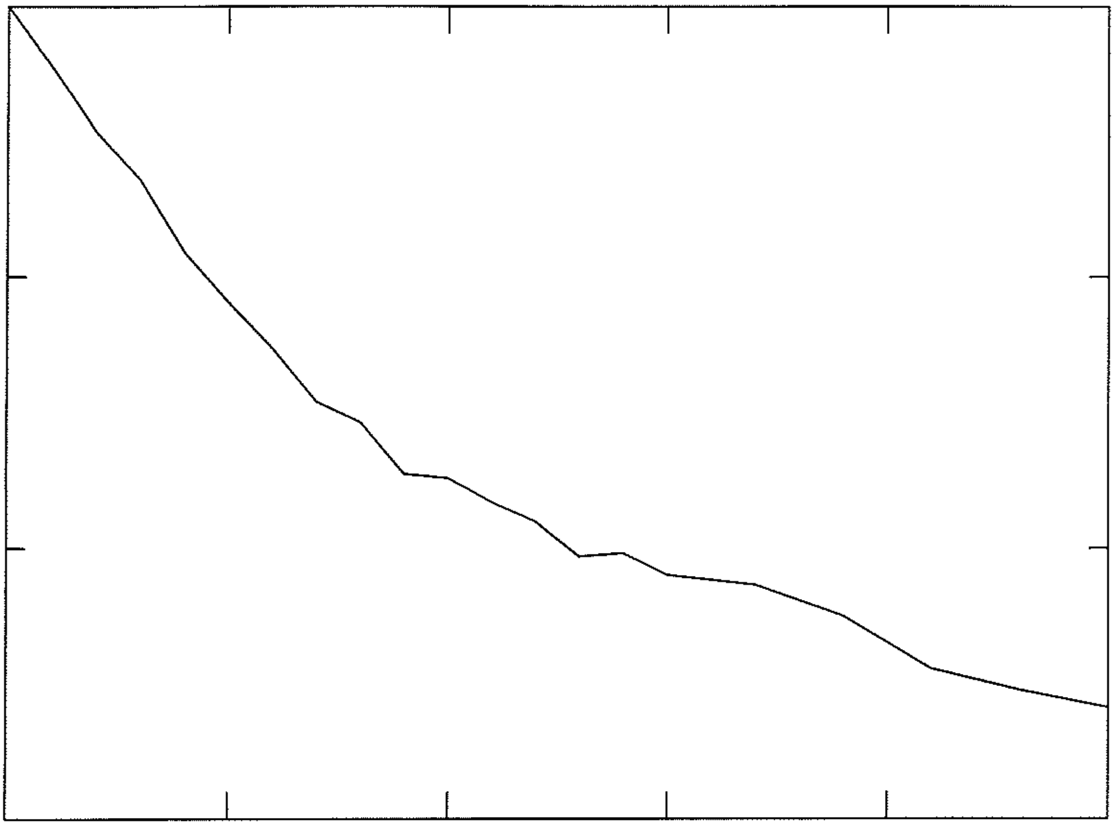

0 -x- 50 0.4 -y- 1

Figure 4; Variation of remanence intensity (y axis), M/Mo, with increasing partial demagnetisation in mT (x axis) for sample 1LBW15.

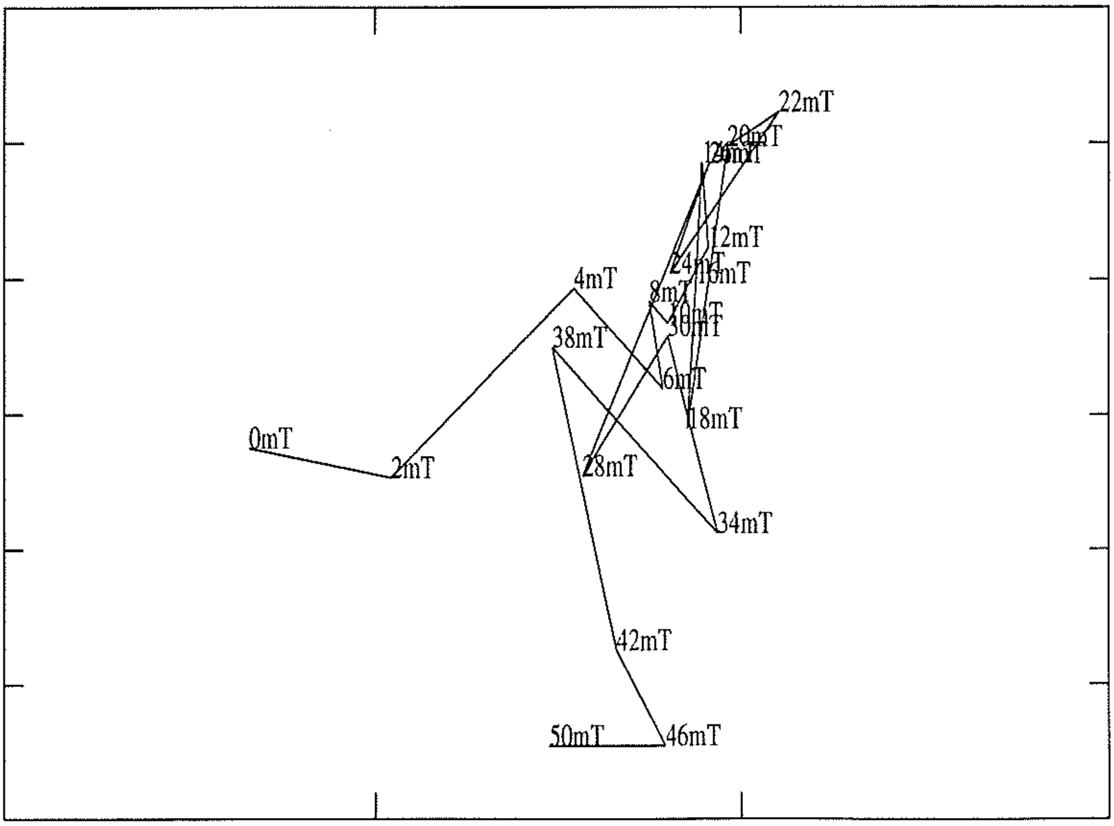

-30 -x- 0 58 -y- 64

Figure 5; Variation of Dec (x axis) and Inc (y axis) with increasing partial demagnetisation for sample 1LBW15.

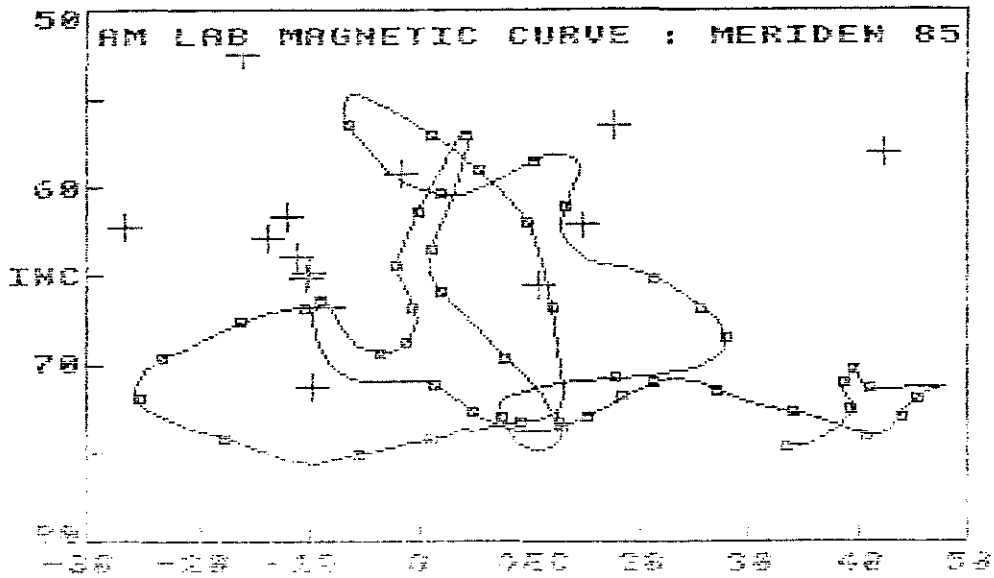

Figure 6; Distribution of partially demagnetised results from feature 1LBW.

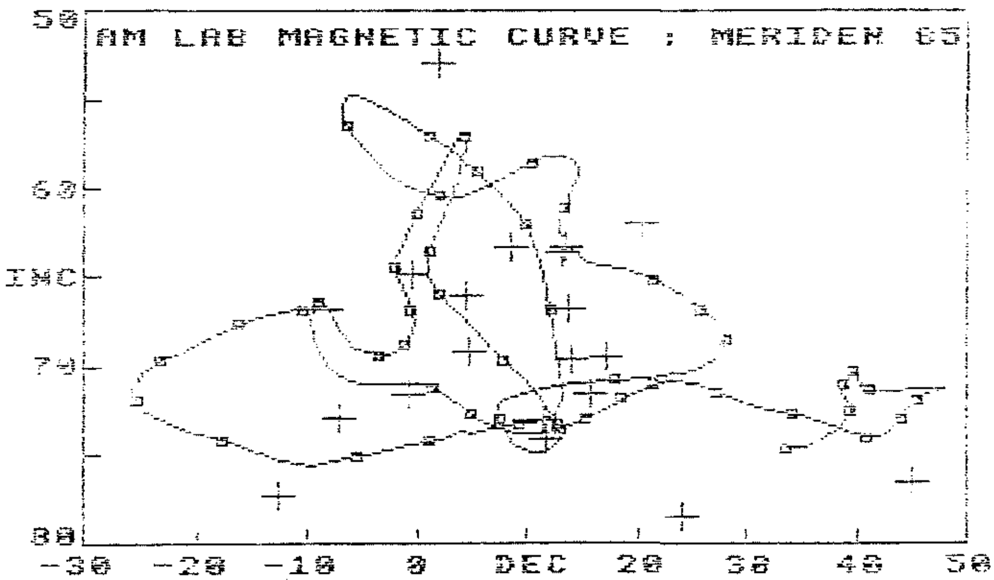

Figure 7; Distribution of NRM results from feature 2LBW.

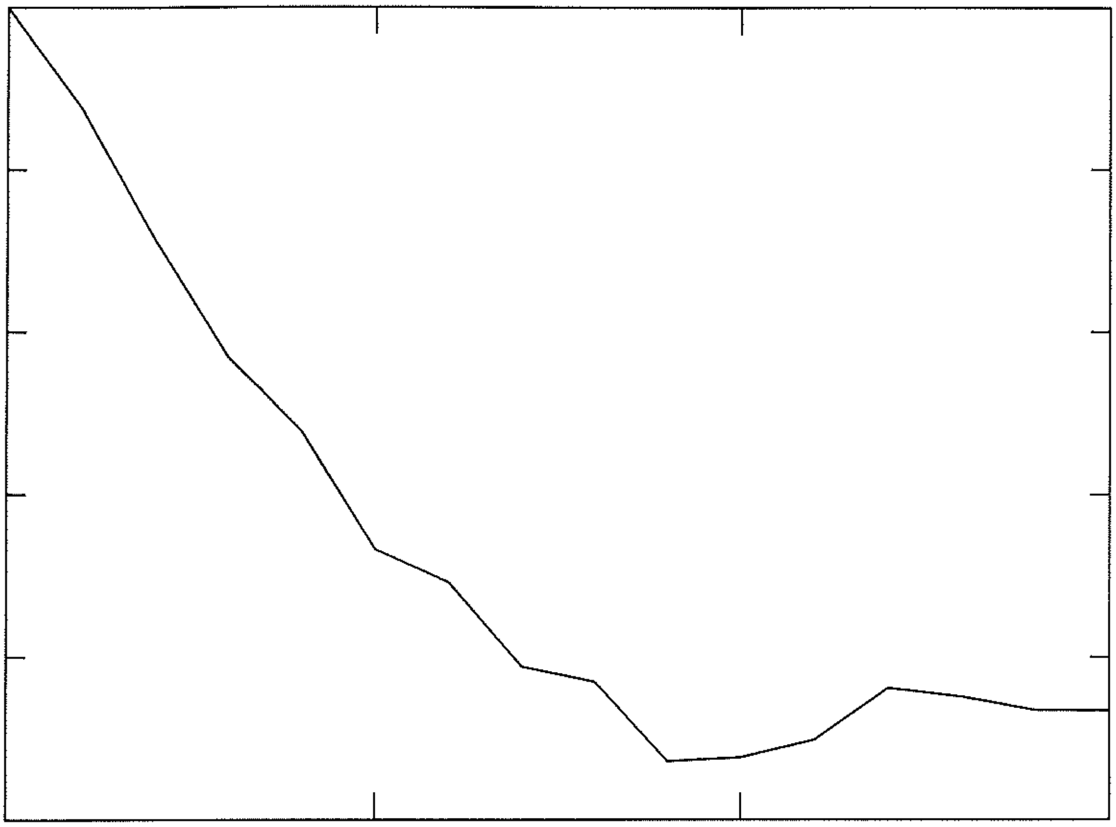

0 -x- 30 0 -y- 1

Figure 8; Variation of remanence intensity (y axis), M/Mo, with increasing partial demagnetisation in mT (x axis) for sample 2LBW07.

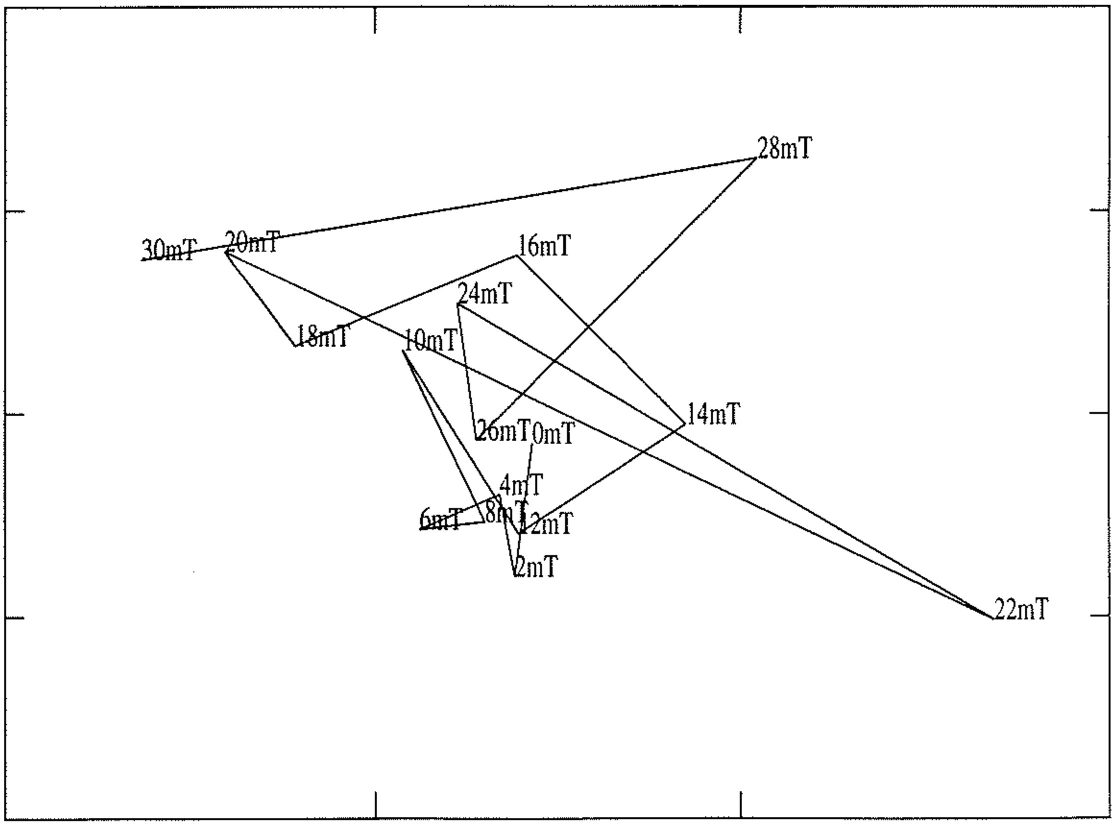

0 -x- 30 55 -y- 75

Figure 9; Variation of Dec (x axis) and Inc (y axis) with increasing partial demagnetisation for sample 2LBW07.

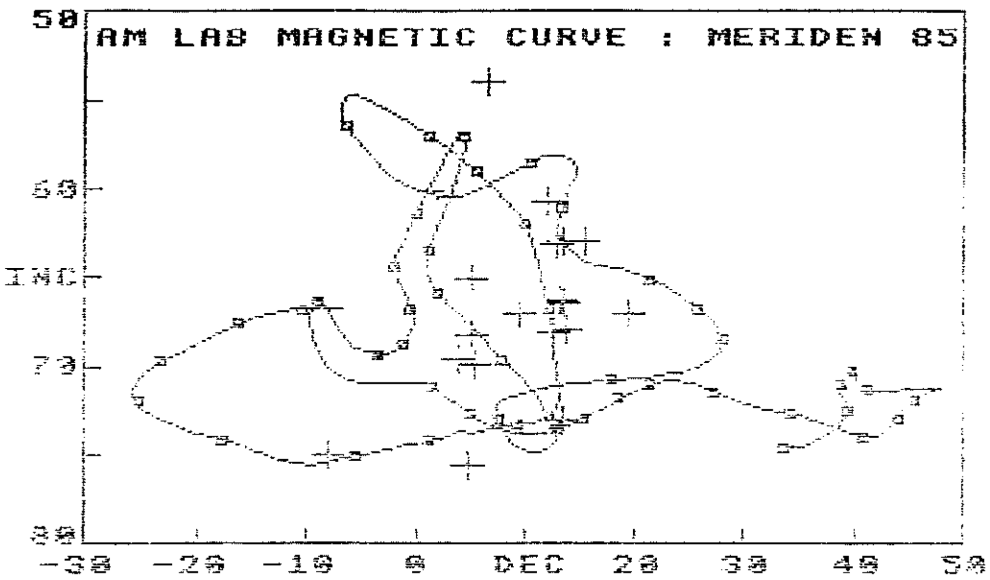

Figure 10; Distribution of partially demagnetised results from feature 2LBW.

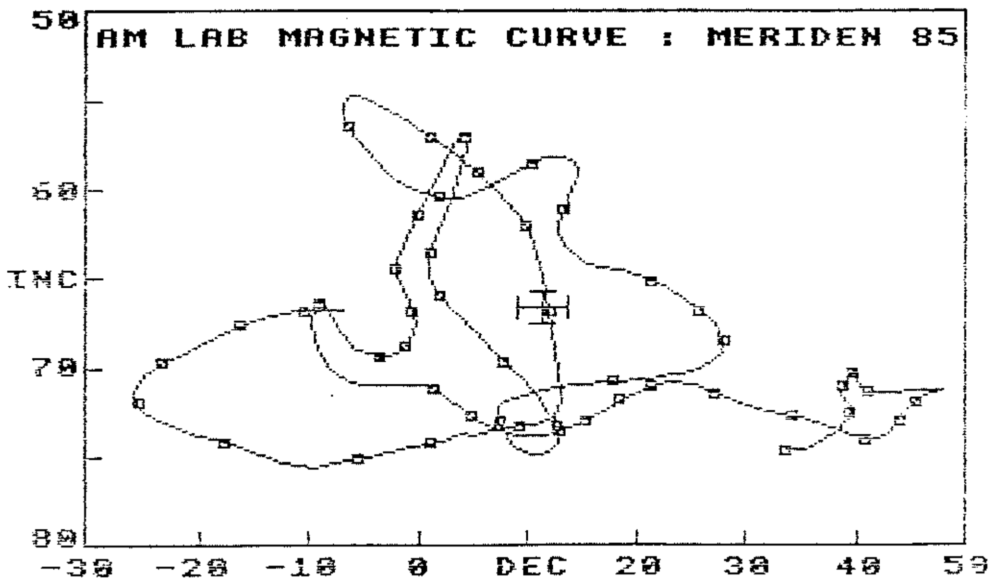

Figure 11; Mean of partially demagnetised results from feature 2LBW with 68% confidence limits.

Appendix: Standard Procedures for Sampling and Measurement

1) Sampling

One of three sampling techniques is employed depending on the consistency of the material (Clark, Tarling and Noel 1988):

a) Consolidated materials: Rock and fired clay samples are collected by the disc method. Several small levelled plastic discs are glued to the feature, marked with an orientation line related to True North, then removed with a small piece of the material attached.

b) Unconsolidated materials: Sediments are collected by the tube method. Small pillars of the material are carved out from a prepared platform, then encapsulated in levelled plastic tubes using plaster of Paris. The orientation line is then marked on top of the plaster.

c) Plastic materials: Waterlogged clays and muds are sampled in a similar manner to method 1b) above; however, the levelled plastic tubes are pressed directly into the material to be sampled.

2) Physical Analysis

a) Magnetic remanences are measured using a slow speed spinner fluxgate magnetometer (Molyneux *et al.* 1972; see also Tarling 1983, p84; Thompson and Oldfield 1986, p52).

b) Partial demagnetisation is achieved using the alternating magnetic field method (As 1967; Creer 1959; see also Tarling 1983, p91; Thompson and Oldfield 1986, p59), to remove viscous magnetic components if necessary. Demagnetising fields are measured in milli-Tesla (mT), figures quoted being for the peak value of the field.

3) Remanent Field Direction

a) The remanent field direction of a sample is expressed as two angles, declination (Dec) and inclination (Inc), both quoted in degrees. Declination represents the bearing of the field relative to true north, angles to the east being positive; inclination represents the angle of dip of this field.

b) Aitken and Hawley (1971) have shown that the angle of inclination in measured samples is likely to be distorted owing to magnetic refraction. The phenomenon is not well understood but is known to depend on the position the samples occupied within the structure. The corrections recommended by Aitken and Hawley are routinely applied to measured inclinations, in keeping with the practise of Clark, Tarling and Noel (1988).

c) Remanent field directions are adjusted to the values they would have had if the feature had been located at Meriden, a standard reference point. The adjustment is done using the method suggested by Noel (Tarling 1983, p116), and allows the remanent directions to be compared with standardised calibration data.

d) Individual remanent field directions are combined to produce the mean remanent field direction using the statistical method developed by R. A. Fisher (1953). The quantity "alpha-95" is quoted with mean field directions and is a measure of the precision of the determination (see Aitken 1990, p247). It is analogous to the standard error statistic for scalar quantities; hence the smaller its value, the better the precision of the date.

4) Calibration

a) Material less than 3000 years old is dated using the archaeomagnetic calibration curve compiled by Clark, Tarling and Noel (1988).

b) Older material is dated using the lake sediment data compiled by Turner and Thompson (1982).

c) Dates are normally given at the 68% confidence level. However, the quality of the measurement and the estimated reliability of the calibration curve for the period in question are not taken into account, so this figure is only approximate. Owing to crossovers and contiguities in the curve, alternative dates are sometimes given. It may be possible to select the correct alternative using independent dating evidence.

d) As the thermoremanent effect is reset at each heating, all dates for fired material refer to the final heating.

e) Dates are prefixed by "cal", for consistency with the new convention for calibrated radiocarbon dates (Mook 1986).

References

Aitken, M. J. 1990. *Science-based Dating in Archaeology*. London: Longman.

Aitken, M. J. and H. N. Hawley 1971. Archaeomagnetism: evidence for magnetic refraction in kiln structures. *Archaeometry* **13**, 83-85.

As, J. A. 1967. The a.c. demagnetisation technique, in *Methods in palaeomagnetism*, D. W. Collinson, K. M. Creer and S. K. Runcorn (eds). Amsterdam: Elsevier.

Clark, A. J., D. H. Tarling and M. Noel 1988. Developments in Archaeomagnetic Dating in Britain. *J. Arch. Sci.* **15**, 645-667.

Creer, K. M. 1959. A.C. demagnetisation of unstable Triassic Keuper Marls from S. W. England. *Geophys. J. R. Astr. Soc.* **2**, 261-275.

Fisher, R. A. 1953. Dispersion on a sphere. *Proc. R. Soc. London A* **217**, 295-305.

Molyneux, L., R. Thompson, F. Oldfield and M. E. McCallan 1972. Rapid measurement of the remanent magnetisation of long cores of sediment. *Nature* **237**, 42-43.

Mook, W. G. 1986. Recommendations/Resolutions Adopted by the Twelfth International Radiocarbon Conference. *Radiocarbon* **28**, M. Stuiver and S. Kra (eds), 799.

Tarling, D. H. 1983. *Palaeomagnetism*. London: Chapman and Hall.

Thompson, R. and F. Oldfield 1986. *Environmental Magnetism*. London: Allen and Unwin.

Turner, G. M. and R. Thompson 1982. Detransformation of the British geomagnetic secular variation record for Holocene times. *Geophys. J. R. Astr. Soc.* **70**, 789-792.